Temperature Dependence of the Ionization Coefficients of $Al_xGa_{1-x}As$

X. G. Zheng, P. Yuan, X. Sun, G. S. Kinsey, A. L. Holmes, B. G. Streetman, and J. C. Campbell

***Abstract*—As $Al_xGa_{1-x}As$ alloys are increasingly used for microwave and millimeter wave power devices and circuits that work under high electric field intensities and junction temperatures; understanding the temperature dependence of impact ionization and related properties in this material system becomes more and more important. Measurements of the multiplication gain and noise of avalanche photodiodes (APDs) provide insight to the avalanche characteristics of semiconductors. Previously, we have reported the characteristics of GaAs and $Al_{0.2}Ga_{0.8}As$ APD's at room temperature. In this paper, the gain and noise of a series of homojunction $Al_xGa_{1-x}As$ APD's were investigated over a wide temperature range from 29 °C to 125 °C, and the temperature dependence of their ionization coefficients was extracted.**

***Index Terms*—Avalanche photodiodes, avalanche multiplication, avalanche noise, ionization coefficients, temperature dependence.**

I. Introduction

SINCE the performance of heterojunction bipolar transistors (HBTs) and high-electron-mobility field-effect transistors (HEMTs) is strongly affected by carrier impact ionization in the high electric field region, the wide application of $Al_xGa_{1-x}As$ in microwave and millimeter-wave power devices and amplifiers requires a thorough understanding of their avalanche properties. Owing to the good lattice match to GaAs substrates, $Al_xGa_{1-x}As$ has also been an important material system for optoelectronic devices. The ionization coefficients of GaAs [1]–[5] and $Al_xGa_{1-x}As$ $(0.1 < x < 0.4)$ [6] have been thoroughly studied and reported. However, the corresponding data for $Al_xGa_{1-x}As$ in a wide temperature range have not been reported.

Since impact ionization requires a high electric-field intensity, it occurs primarily in the lightly doped region of most III–V-semiconductor power devices. Under normal operating conditions, the collector region of HBTs and the substrate region under the drain-substrate interface of HEMTs and MESFETs are usually lightly doped and the bias is high. In these cases, the conventional local-field avalanche theory [7]–[13] has proved very successful in describing impact ionization characteristics. The basic assumption of the local-field theory is that impact ionization is a continuous and local process and that the impact ionization probability of carriers in a material is only a function of local electric field, irrespective of a carrier's previous ionization history. Although this theory is inaccurate and thus no longer applicable when the multiplication region is thin (<0.5 μm) [14]–[24], it is still useful for thick structures, which applies to most high power transistors and many optoelectronics devices.

The two common methods that have been utilized to determine the ionization coefficients of materials have been described thoroughly by Stillman *et al.* [1]. These techniques are based on comparisons of the gain under pure electron injection and hole injection. Since the two gain curves are often quite close to each other and the extraction of the coefficients depends on the difference between the two, the accuracy of the final result is subject to the influence of many factors in the experiment. In order to avoid deviations caused by variations in crystal growth, it is preferable if the two gain curves can be measured on the same device. This requirement can be satisfied with heterojunction structures, however, this often results in a higher-than-zero punch-through voltage, which, in turn, makes it more difficult to determine the unity-gain reference. It is in this context that we have used gain and noise measurements under pure electron injection to determine the ionization coefficients of electrons and holes for the case where the local-field avalanche theory is effective. In this study, a series of homojunction GaAs and $Al_xGa_{1-x}As$ APD's with different aluminum ratios and 0.8-μm-thick multiplication regions were fabricated. Their ionization coefficients over a temperature range from 29 °C to 125 °C have been extracted from measurements of the gain for electron injection and the excess noise factor using the local-field model, which is adequate for the 0.8-μm-thick multiplication regions that were used in this study.

Throughout this paper, all assumptions and analysis are based on the local-field avalanche theory [1], [7]–[13]. For simplicity, a one-dimensional avalanche diode model is adopted, and for the discussion, it is assumed that the n^+, i, and p^+ regions are arranged from left to right. The origin of coordinates is placed at the interface between the n^+ and i regions, and the thickness of the i region is w. Under reverse bias, electrons are swept from right to left and holes from left to right.

II. Theory Review

For the homojunction APD's studied here, the background doping is low ($\sim 2 \times 10^{15}$ cm^{-3}) in the "i" region and the p^+ and n^+ layers are heavily doped ($>10^{18}$ cm^{-3}). Consequently, the electric field intensity in the i region is approximately flat and its extension into the p^+ and n^+ regions can be ignored.

Manuscript received March 29, 2000; revised June 19, 2000. This work was supported by Motorola under Contract MOTO UTA00-046 and by the DARPA-sponsored Heterogeneous Optoelectronic Technology Center.

The authors with the Microelectronics Research Center, Department of Electrical and Computer Engineering, The University of Texas at Austin, Austin, TX 78712 USA.

Publisher Item Identifier S 0018-9197(00)08148-3.

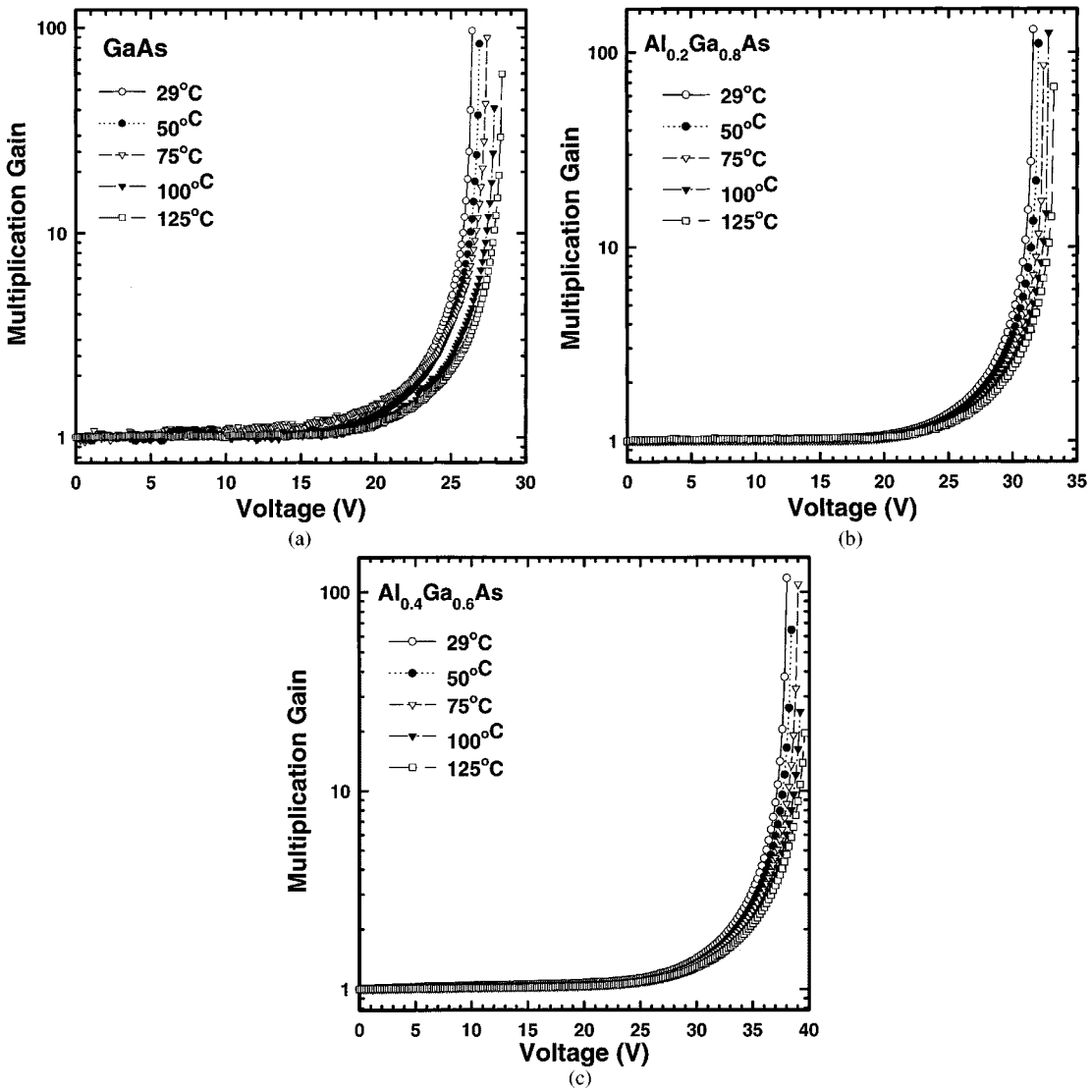

Fig. 1. The measured gains for: (a) GaAs; (b) $Al_{0.2}Ga_{0.8}As$; and (c) $Al_{0.4}Ga_{0.6}As$ APD's at specified temperatures.

Since the ionization coefficient $(\alpha(E))$ of electrons is greater than that of holes $(\beta(E))$ in GaAs and $Al_xGa_{1-x}As$, the PIN structure has been designed to ensure that essentially all of the incident photons are absorbed in the top p layer. This provides pure electron injection into the multiplication region, which results in the lowest noise and highest gain. For the local-field model, the ratio of α and β is treated as a constant $k = \beta/\alpha$. For these conditions, the gain can be expressed in terms of k and α as

$$M_e = \frac{1}{1 - \frac{1}{1-k}[1 - \exp(-w\alpha(1-k))]}. \tag{1}$$

The noise power spectral density S (with units of W/Hz) is

$$S = 2eI_0M^2F(M)R(\omega) \tag{2}$$

where

$$F(M) = kM + (1-k)\left(2 - \frac{1}{M}\right). \tag{3}$$

In the above equations, I_0 is the injected electron photocurrent, e is the electron charge, $R(\omega)$ is the impedance of the circuit, and $F(M)$ is the excess noise factor. For each value of M, a value of k was determined using (3) and the measured excess noise, $F(M)$. Combined with the gain curve obtained from the IV measurement, the ionization coefficients for a specific M (and thus E) were calculated using the relations

$$\alpha = \frac{-\ln\left[1 - \frac{(M_e-1)\cdot(1-k)}{M_e}\right]}{(1-k)\cdot w}. \tag{4}$$

$$\beta = k \cdot \alpha. \tag{5}$$

The ionization coefficients are frequently expressed as follows:

$$\alpha(E) = A_e \cdot \exp\left(-\frac{E_{c,e}}{E}\right) \tag{6}$$

$$\beta(E) = A_h \cdot \exp\left(-\frac{E_{c,h}}{E}\right) \tag{7}$$

where E is the electric field and $A_e, A_h, E_{c,e}$ and $E_{c,h}$ are empirical constants.

III. Materials Growth and Device Fabrication

The $Al_xGa_{1-x}As$ APD's in the present work utilized 0.8-μm-thick multiplication regions and different Al ratios ($x = 0.0, 0.2$, and 0.4). The wafers were grown in a Varian GEN-II MBE reactor on n^+ GaAs substrates. Reflection high-energy electron diffraction measurements were employed to calibrate the thickness of each layer during MBE growth. Since APDs operate at high electric field intensities, any defects in the multiplication region can cause premature breakdown (through microplamas) and/or high dark current. In addition, low contact resistance is necessary in order to minimize the noise and to achieve stable results. In the APD structures, the i layers were sandwiched between a 1500-nm-thick p^+ layer on the top and a 200-nm-thick n^+ layer below. The i region was nominally undoped with a background n-type doping concentration approximately 2×10^{15} cm^{-3}, while the doping in the p and n layer varied from 1×10^{18} cm^{-3} to 4×10^{18} cm^{-3}. Little difference was found between the nominal design thickness and the values that were determined from C-V measurements. In order to insure a good p contact, a layer of 30-nm-thick heavily doped ($>10^{19}$ cm^{-3}) p^+ GaAs layer was grown on the top.

Mesas with a diameter of 60 μm were formed by etching in a H_2SO_4:H_2O_2:H_2O (1:1:10) solution. The ohmic contacts were patterned using a standard photolithography and liftoff process. Au-Cr metal served as the p contact and Ni-AuGe-Au was used as the n contact. In order to minimize the contact resistance, the n contact covered the whole surface of the wafer except the mesa areas. After the metal deposition, annealing was performed in nitrogen ambient at 450 °C for 30 s. More details of the growth and process can be found in [19].

IV. Measurements and Parameter Extraction

Two stable continuous-wave (cw) lasers, an Nd:YAG laser (5 mW, $\lambda = 532$ nm), and an Argon UV laser (500 mW, $\lambda = 351$ nm and 363 nm), were employed in the measurements in order to control the optical absorption length in different materials. The GaAs and $Al_{0.2}Ga_{0.8}As$ devices were measured with the Nd:YAG laser, and the $Al_{0.4}Ga_{0.6}As$ devices were measured with UV illumination. In order to avoid mixed injection, the beams were carefully focused onto the top of the device mesa via a microscope objective, in front of which an iris was placed to shield all but the central beam. A small focal spot and a large working distance were obtained for the 532-nm beam with a $40x$ Zeiss UD objective. A UV objective $(10x)$ was essential to alleviate the insertion loss in the UV region. We estimate that the worst hole contamination occurs in the $Al_{0.2}Ga_{0.8}As$ devices. Based on the published absorption coefficient data [25], we estimate that the photon "leakage" through the 1.5-μm-thick $Al_{0.2}Ga_{0.8}As$ top p layer is approximately 0.16%, and the reflection of the semiconductor-air interface is approximately 30%. Therefore, only about 0.11% of the incident photons are absorbed beyond the p region in the i layer. Since the hole injection efficiency of these survival photons is far from unity and the total external quantum efficiency of the device is approximately 5%, we conservatively estimate that the fraction of hole injection in the $Al_{0.2}Ga_{0.8}As$ devices is below 2%. In order to control the temperature, the test wafers were mounted on a thermoelectric heater and the temperature was monitored with a thermal-couple.

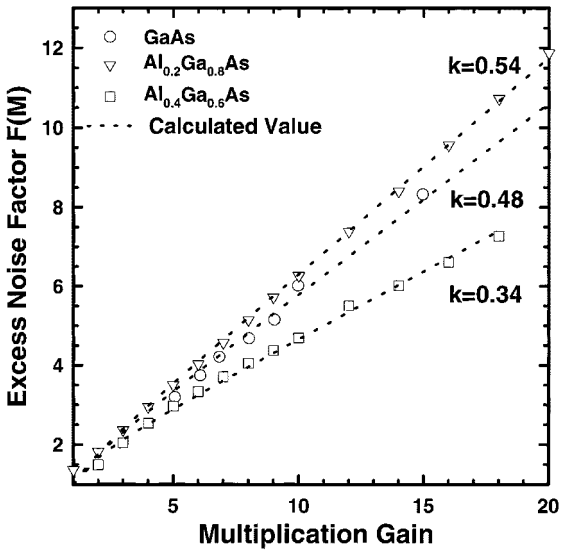

Fig. 2. The room-temperature excess noise factors of the GaAs, $Al_{0.2}Ga_{0.8}As$, and $Al_{0.4}Ga_{0.6}As$ APDs. The symbols show the measured excess noise factors, the dotted lines are the calculated values obtained by using (6) and the specified k's.

The unity-gain reference current, I_{unity}, was measured at low bias where the photocurrent is flat, independent of voltage. The photocurrent for higher bias voltages was determined by measuring the total current I_{total}, under the same illumination, and subtracting the dark current I_{dark}. The avalanche gain $M(V)$ as a function of voltage was then calculated using the relation

$$M(V) = \frac{I_{\text{total}} - I_{\text{dark}}}{I_{\text{unity}}}. \tag{8}$$

All of the devices measured achieved maximum multiplication gains of at least 30. The dark currents were usually less than 10 pA at 90% of the breakdown voltage. Fig. 1 shows the variation of the gain with temperature in the range 29 °C $< T <$ 125° 125 °C. Due to increased phonon scattering, the acceleration of carriers becomes less effective at a higher temperature. As a result, the mean free path between ionization events increases and the gain decreases with temperature.

The noise power spectral density was measured at 50 MHz with a bandwidth of 4 MHz with an HP 8970B noise figure meter. A preamplifier was used between the APD and the noise figure meter. The gain of the preamplifier was carefully chosen to avoid transient saturation. In order to eliminate the environmental noise and any signal resonance in the transmission line, the devices were contacted with a shielded microwave probe. The noise of all the components following the photodiode was calibrated and normalized with a standard noise source. In order to determine the coefficient $2eR(\omega)$ in (2), the shot noise of the photodiode at unity gain was measured as a function of photocurrent. This calibration step is essential because the impedance and the contact resistance vary from device to device, especially over a wide temperature range. The avalanche noise power density was measured as a function of

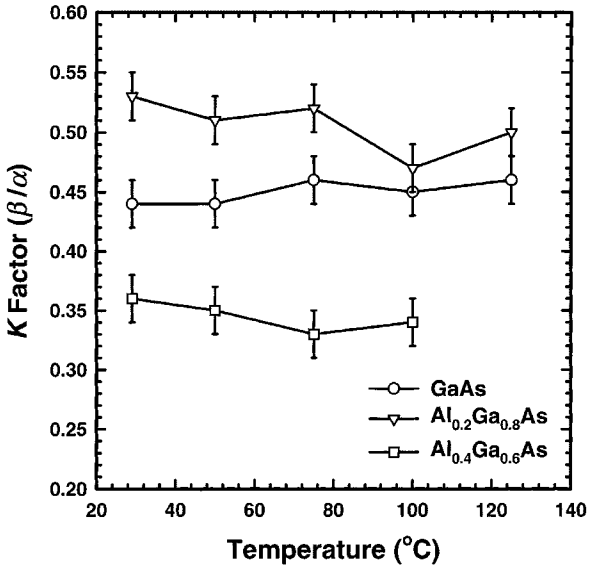

Fig. 3. Temperature dependence of the k values fitted with the measured excess noise factors of the 0.8-μm-thick homojunction $Al_xGa_{1-x}As$ APDs.

gain under illumination and in the dark. Fig. 2 shows the excess noise factors $F(M)$ extracted from the noise measurements for all the devices at room temperature. The dashed lines are fits to $F(M)$ using k as an adjustable parameter in (2) and (3). The temperature dependence of k for all three materials is shown in Fig. 3. From these plots, it is clear that for the materials studied in this paper, k changes little with temperature within the accuracy of the experiment.

From the gain curves shown in Fig. 1, the relationship of the gain M_e and the electric field E can be easily calculated. Combined with the ionization coefficient ratios obtained in the noise measurement, the ionization coefficients $\alpha(E)$ and $\beta(E)$ can be calculated using (4) and (5). In Fig. 4, the ionization coefficients of GaAs, $Al_{0.2}Ga_{0.8}As$ and $Al_{0.4}Ga_{0.6}As$ are plotted versus E^{-1}. The constants in (6) and (7) have been determined by fitting the ionization coefficient curves in Fig. 4. The parameters for each material are listed in Table I.

The temperature dependence of the ionization coefficients of GaAs has been reported by Capasso *et al.* in 1977 [2] and by Robbins *et al.* in 1988 [4]–[6]. Table II compares those results with the present work. It should be noted that there are significant differences in the material growth methods, device fabrication techniques, device structures, and measurement techniques employed in this work and those of Capasso *et al.* and Robbins *et al.*

Capasso et al. reported the measurements of ionization coefficients of GaAs from 29 °C to 250 °C. They investigated the ionization coefficients of GaAs by means of abrupt P^+N homojunction diodes ($p \approx 2 \times 10^{18}$ cm^{-3} and $n \approx 2 \times 10^{18}$ cm^{-3}, respectively) at a wavelength of 633 nm and impact ionization region greater than 1-μm thick. They observed that the ionization coefficients of holes and electrons decrease with increasing temperature as a result of increased phonon scattering. They reported that the ionization coefficient of electrons and holes were approximately equal with β slightly greater than α, and that the k factor was relatively insensitive to the temperature change.

TABLE I
PARAMETERS FOR THE IONIZATION COEFFICIENTS IN $Al_xGa_{1-x}As$ ($x = 0.0, 0.2, 0.4$) FOR THE TEMPERATURE RANGE 29 °C–125 °C

Materials	Temperature (°C)	A_e ($10^6 cm^{-1}$)	$E_{c,e}$ ($10^6 V/cm$)	A_h ($10^6 cm^{-1}$)	$E_{c,h}$ ($10^6 V/cm$)
GaAs	29	1.94	1.58	0.85	1.58
	50	1.73	1.58	0.76	1.58
	75	0.291	1.03	0.134	1.03
	100	3.16	1.83	1.42	1.83
	125	3.44	1.90	1.58	1.90
$Al_{0.2}Ga_{0.8}As$	29	3.17	2.10	1.68	2.10
	50	4.34	2.25	2.21	2.25
	75	8.17	2.52	4.25	2.52
	100	2.99	2.17	1.41	2.17
	125	4.83	2.38	2.41	2.38
$Al_{0.4}Ga_{0.6}As$	29	2.49	2.37	0.897	2.37
	50	3.83	2.59	1.34	2.59
	75	2.70	2.46	0.892	2.46
	100	3.21	2.58	1.09	2.58

TABLE II
COMPARISON OF TEMPERATURE DEPENDENCE OF IONIZATION COEFFICIENTS (α, β), FOR AN ELECTRIC FIELD INTENSITY OF 4.3×10^6 V/CM WITHIN THE IMPACT IONIZATION REGION, WITH THOSE OF CAPASSO *ET AL.* [2], AND THOSE EXTRACTED FROM THE EXPERIMENTAL RESULTS OF ROBBINS *ET AL.* [4]–[6]

Reference [2]

	29 °C	100 °C	150 °C	200 °C	250 °C
α ($10^4$1/cm)	3.0	2.1	1.55	1.5	1.3
β ($10^4$1/cm)	3.2	2.4	2.0	1.4	1.0

References [4-6]

	27 °C	77 °C	117 °C	157 °C	192 °C
α ($10^4$1/cm)	4.0	3.2	2.8	2.9	3.0
β ($10^4$1/cm)	3.4	2.8	2.2	2.0	1.9

Present Work

	29 °C	50 °C	75 °C	100 °C	125 °C
α ($10^4$1/cm)	6.5	6	4.5	4.0	4.0
β ($10^4$1/cm)	2.9	2.5	2.1	2.0	1.9

The results presented here are in better agreement with those of Robbins et al., both the temperature dependence of the ionization coefficients of GaAs within the temperature range from 29 °C to 125 °C and the ionization coefficients of $Al_xGa_{1-x}As$ (with x from 0 to 0.4) at room temperature. Also, the temperature dependence of hole ionization coefficients

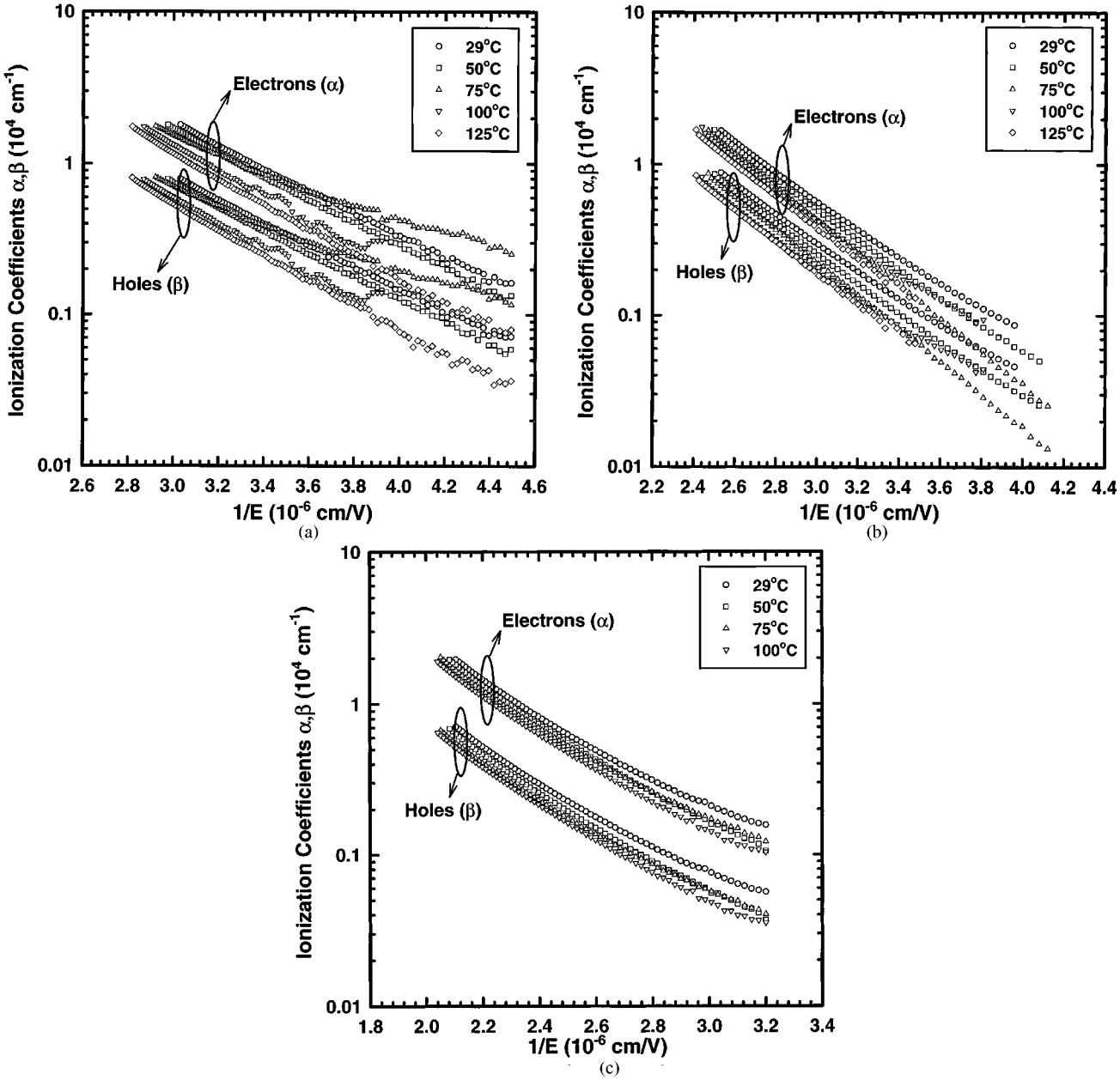

Fig. 4. Ionization coefficients of (a) GaAs, (b) $Al_{0.2}Ga_{0.8}As$, and (c) $Al_{0.4}Ga_{0.6}As$ at different temperatures.

agrees fairly well with the results of Robbins *et al*. The decrease of ionization coefficients with increasing Al concentration reflects the increase in the band gap and, hence, an increase in the threshold energy for impact ionization. The ionization coefficients of $Al_xGa_{1-x}As$ exhibited the same temperature trends as those of GaAs. From the present results, we conclude that while the ionization coefficients of GaAs and $Al_xGa_{1-x}As$ $(0 \leq x \leq 0.4)$ decrease with increasing temperature, the temperature dependence in the range 29 °C to 125 °C is not strong and the k values are relatively constant.

V. Conclusion

The ionization characteristics of $Al_xGa_{1-x}As$ $(x = 0.0$–$0.4)$ for high electric field have been investigated within the temperature range 29 °C to 125 °C. A series of $Al_xGa_{1-x}As$ APD's with 800-nm-thick multiplication regions were grown and processed. The gain and noise spectral density of these devices were measured versus temperature. With the measured gains and excess noise factors, the ionization coefficients were calculated in a specific electric-field region, and the ionization parameters were calculated using the conventional ionization coefficient model. It was found that the ionization coefficient ratios of different $Al_xGa_{1-x}As$ alloys do not change significantly within a wide range of temperature (29 °C–125 °C). Due to the temperature dependence of phonon scattering, the ionization coefficients decrease slightly as the working temperature increases.

Acknowledgment

The authors would also like to thank T. Li and S. Wang for many useful discussions.

REFERENCES

[1] G. E. Stillman and C. M. Wolfe, "Avalanche Photodiodes," *Semiconductors and Semimetals*, vol. 12, 1977.

[2] F. Capasso, R. E. Nahory, M. A. Pollack, and T. P. Pearsall, "Observation of electronic band-structure effects on impact ionization by temperature tuning," *Phys. Rev. Lett.*, vol. 39, no. 11, pp. 723–726, 1977.

[3] F. Capasso, R. E. Nahory, and M. A. Pollack, "Temperature dependence of impact ionization rates in GaAs between 20 degrees and 200 degrees C," *Electron. Lett.*, vol. 15, no. 4, pp. 117–118, 1979.

[4] G. E. Bulman, V. M. Robbin, K. F. Brennan, K. Hess, and G. E. Stillman, "Experimental determination of impact ionization coefficients in (100) GaAs," *IEEE Electron Device Lett.*, vol. EDL-4, pp. 181–185, June 1983.

[5] G. E. Bulman, V. M. Robbin, and G. E. Stillman, "The determination of impact ionization coefficients in (100) gallium arsenide using avalanche noise and photocurrent multiplication measurements," *IEEE Trans. Electron Device*, vol. ED-32, pp. 2454–2466, Nov. 1985.

[6] V. M. Robbins, S. C. Smith, and G. E. Stillman, "Impact ionization in $Al_xGa_{1-x}As$ for $x = 0.1$–0.4," *Appl. Phys. Lett.*, vol. 52, no. 4, pp. 2996–2998, 1988.

[7] N. R. Howard, *J. Electron. Contr.*, vol. 13, p. 537, 1962.

[8] C. A. Lee, R. A. Logan, R. L. Batdorf, J. J. Kleimack, and W. Wiegmann, "Ionization rates of holes and electrons in silicon ," *Phys. Rev.*, vol. 134, pp. A761–A763, 1964.

[9] R. J. McIntyre, "Multiplication noise in uniform avalanche diodes," *IEEE Trans. Electron Devices*, vol. ED-13, Jan. 1966.

[10] ——, "The distribution of gains in uniformly multiplying avalanche photodiodes: Theory," *IEEE Trans. Electron Devices*, vol. ED-19, pp. 703–713, 1972.

[11] ——, "Factors affecting the ultimate capabilities of high speed avalanche photodiodes and a review of the state-of-the-art," *Tech. Dig. Int. Electron Device Mtg.*, pp. 213–216, 1973.

[12] R. B. Emmons, "Avalanche-photodiode frequency response," *J. Appl. Phys.*, vol. 38, no. 9, pp. 3705–3714, 1967.

[13] R. B. Emmons and G. Lucovsky, "The frequency response of avalanching photodiodes," *IEEE Trans. Electron Devices*, vol. ED-13, pp. 297–305, Mar. 1966.

[14] J. C. Campbell, S. Chandrasekhar, W. T. Tsang, G. J. Qua, and B. C. Johnson, "Multiplication noise of wide-bandwidth InP/InGaAsP/InGaAs avalanche photodiodes," *J. Lightwave Technol.*, vol. 7, no. 3, pp. 473–477, Mar. 1989.

[15] C. Hu, K. A. Anselm, B. G. Streetman, and J. C. Campbell, "Noise characteristics of thin multiplication region GaAs avalanche photodiodes," *Appl. Phys. Lett.*, vol. 69, no. 24, pp. 3734–3736, Dec. 1996.

[16] K. F. Li, D. S. Ong, J. P. R. David, G. J. Rees, R. C. Tozer, P. N. Robson, and R. Grey, "Avalanche multiplication noise characteristics in thin GaAs p^+-i-n^+ diodes," *IEEE Trans. Electron Devices*, vol. 45, pp. 2102–2107, Oct. 1998.

[17] K. F. Li, D. S. Ong, J. P. R. David, R. C. Tozer, G. J. Rees, P. N. Robson, and R. Grey, "Low excess noise characteristics in thin avalanche region GaAs diodes," *Electron. Lett.*, vol. 34, no. 1, p. 125, 1997.

[18] R. J. McIntyre, "A new look at impact ionization—Part I: A theory of gain, noise, breakdown probability, and frequency response," *IEEE Trans. Electron Devices*, vol. 46, pp. 1623–1631, Aug. 1999.

[19] P. Yuan, K. A. Anselm, C. Hu, H. Nie, C. Lenox, A. L. Holmes, B. G. Streetman, J. C. Campbell, and R. J. McIntyre, "A new look at impact ionization—Part II: Gain and noise in short avalanche photodiodes," *IEEE Trans. Electron Devices*, vol. 46, pp. 1632–1639, Aug. 1999.

[20] K. M. van Vliet, A. Friedmann, and L. M. Rucker, "Theory of carrier multiplication and noise in avalanche devices—Part II: Two-carrier processes," *IEEE Trans. Electron Devices*, vol. ED-26, pp. 752–764, 1979.

[21] J. S. Marsland, "On the effect of ionization dead spaces on avalanche multiplication and noise for uniform electric field," *J. Appl. Phys.*, vol. 67, pp. 1929–1933, 1990.

[22] M. M. Hayat, B. E. A. Saleh, and M. C. Teich, "Effects of dead space on gain and noise of double-carrier-multiplication avalanche photodiodes," *IEEE Trans. Electron Devices*, vol. 39, pp. 546–552, 1992.

[23] M. M. Hayat, W. L. Sargent, and B. E. A. Saleh, "Effect of dead space on gain and noise in Si and GaAs avalanche photodiodes," *IEEE J. Quantum Electron.*, vol. 28, pp. 1360–1365, 1992.

[24] J. S. Marsland, R. C. Woods, and C. A. Brownhill, "Lucky drift estimation of excess noise factor for conventional avalanche photodiodes including the dead space effect," *IEEE Trans. Electron Devices*, vol. 39, pp. 1129–1134, 1992.

[25] D. E. Aspnes, S. M. Kelso, R. A. Logan, and R. Bhat, "Optical properties of $Al_xGa_{1-x}As$," *J. Appl. Phys.*, vol. 60, pp. 754–767, July 1986.

X. G. Zheng, photograph and biography not available at time of publication.

P. Yuan, photograph and biography not available at time of publication.

X. Sun, photograph and biography not available at time of publication.

G. S. Kinsey, photograph and biography not available at time of publication.

A. L. Holmes, photograph and biography not available at time of publication.

B. G. Streetman, photograph and biography not available at time of publication.

J. C. Campbell, photograph and biography not available at time of publication.